ORIGINAL ARTICLE

JBMR

Near-Infrared Fluorescent Probe Traces Bisphosphonate Delivery and Retention In Vivo

Kenneth M Kozloff,[1,3] Leo I Volakis,[1,3] Joan C Marini,[2] and Michelle S Caird[1]

[1]Orthopaedic Research Laboratories, Department of Orthopaedic Surgery, University of Michigan, Ann Arbor, MI, USA
[2]Bone and Extracellular Matrix Branch, NICHD, NIH, Bethesda MD
[3]Department of Biomedical Engineering, University of Michigan, Ann Arbor, MI, USA

ABSTRACT

Bisphosphonate use has expanded beyond traditional applications to include treatment of a variety of low-bone-mass conditions. Complications associated with long-term bisphosphonate treatment have been noted, generating a critical need for information describing the local bisphosphonate-cell interactions responsible for these observations. This study demonstrates that a fluorescent bisphosphonate analogue, far-red fluorescent pamidronate (FRFP), is an accurate biomarker of bisphosphonate deposition and retention in vivo and can be used to monitor site-specific local drug concentration. In vitro, FRFP is competitively inhibited from the surface of homogenized rat cortical bone by traditional bisphosphonates. In vivo, FRFP delivery to the skeleton is rapid, with fluorescence linearly correlated with bone surface area. Limb fluorescence increases linearly with injected dose of FRFP; injected FRFP does not interfere with binding of standard bisphosphonates at the doses used in this study. Long-term FRFP retention studies demonstrated that FRFP fluorescence decreases in conditions of normal bone turnover, whereas fluorescence was retained in conditions of reduced bone turnover, demonstrating preservation of local FRFP concentration. In the mandible, FRFP localized to the alveolar bone and bone surrounding the periodontal ligament and molar roots, consistent with findings of osteonecrosis of the jaw. These findings support a role for FRFP as an effective in vivo marker for bisphosphonate site-specific deposition, turnover, and long-term retention in the skeleton.

KEY WORDS: BISPHOSPHONATES; MOLECULAR IMAGING; FLUORESCENCE; OSTEOGENESIS IMPERFECTA; OSTEONECROSIS OF THE JAW

Introduction

Bisphosphonates are a class of drugs used traditionally to treat adult diseases of high bone turnover, such as osteoporosis, Paget disease, myeloma, and metastatic bone disease.[1] Bisphosphonates bind directly to mineralized bone surfaces, where they are taken up by osteoclasts and inactivate osteoclast activity. The resulting reduction in bone resorption leads to a net positive bone balance.[2] Recently, the use of bisphosphonates has been expanding in children and adolescents to treat a variety of pediatric osteopenic conditions, including fibrous dysplasia, traumatic osteonecrosis of the femoral head, disuse osteopenia, and osteogenesis imperfecta (OI).[3–6]

Despite a history of use in adult and pediatric populations, recent complications have led to calls urging caution for long-term bisphosphonate use. Low-energy fractures have been reported in osteoporotic patients treated with bisphosphonates, possibly resulting from reduced remodeling of microdamage in bone[7] or from altered material properties.[8,9] OI patients treated with bisphosphonates have shown delayed healing of osteotomy sites,[10] delayed tooth eruption,[11] and a remarkable osteosclerotic phenotype in metaphyseal bone reflecting treatment during a growth period.[12–15] In a mouse model for OI, bisphosphonate treatment improves bone size, but bending strength fails to increase to proportional levels, and bones remain brittle.[16] In patients treated with high bisphosphonate doses during cancer treatment, osteonecrosis of the jaw (ONJ) has emerged as a serious complication, with exposed bone in the maxillofacial region that persists for at least 8 weeks.[17–21] Together these findings suggest a critical need for information describing local drug-cell interactions within the skeleton. Developing biomarkers for bisphosphonate deposition and retention would be valuable to understand these findings.[18]

Received in original form October 15, 2009; revised form January 6, 2010; accepted February 3, 2010. Published online February 8, 2010.
Address correspondence to: Kenneth M Kozloff, PhD, 2015 Biomedical Science Research Building, 109 Zina Pitcher Place, Ann Arbor, MI 48109-2200, USA.
E-mail: kenkoz@umich.edu
This manuscript was presented in part at the 2009 Orthopaedic Research Society Meeting, February 22–25, 2009, Las Vegas, NV, and the 2009 Summer ASME-BED Meeting, June 17–21, 2009, Lake Tahoe, CA.

Journal of Bone and Mineral Research, Vol. 25, No. 8, August 2010, pp 1748–1758
DOI: 10.1002/jbmr.66

Bisphosphonates tagged with radionucleotides have been used as short-term markers of bisphosphonate deposition and localization in the skeleton. However, a short half-life prevents these drugs from being useful for long-term studies of retention posttreatment. Long-term retention of bisphosphonates within the skeleton has been observed by urinary excretion markers for up to 8 years after cessation of treatment in youths with severe osteoporosis.[22] While this method of observation demonstrates long-term retention, it fails to provide site-specific information on local drug concentration. Site-specific binding of bisphosphonates to metabolically active areas in the growing skeleton has been inferred by the correlation of osteosclerotic lines with the number and frequency of bisphosphonate treatment cycles in growing patients.[23] However, direct verification of this association has yet to be proven. Furthermore, if bisphosphonates retain their antiresorptive capacity over extended periods of time in the skeleton, direct visualization of areas that retain high bisphosphonate concentrations will be important to understanding their effect on subsequent healing of damaged tissue.

Recently, the functionalization of the bisphosphonate pamidronate with a near-infrared fluorophore has been developed and characterized.[24,25] This far-red fluorescent pamidronate (FRFP) has been used as a tool for monitoring bone turnover and repair[24–26] and extraskeletal calcification in vivo.[25,27–29] Similar fluorescent bisphosphonate probes have been used to monitor bisphosphonate-osteoclast interactions in vitro.[30] Using a near-infrared imaging strategy allows for deep signal penetration through tissues in a region of the spectrum where tissue autofluorescence is low, providing high signal-to-noise values.[31] Despite demonstration of this imaging strategy in a variety of disease contexts, the potential of FRFP as a tracer compound for bisphosphonate delivery and retention in vivo has yet to be established. Use of FRFP as an in vivo bisphosphonate marker would provide a noninvasive, repeatable methodology capable of directly visualizing the deposition and long-term retention or release of bisphosphonate from the skeleton. This study validates a fluorescent bisphosphonate analogue as a biomarker for bisphosphonate deposition and retention in vivo to monitor local drug concentration in a site-specific manner.

Materials and Methods

In vivo imaging probes

FRFP680 and FRFP750 (Osteosense, VisEn Medical, Bedford, MA, USA) have nonoverlapping excitation (680 and 750 nm) and emission (700 and 780 nm) peaks to allow for multichannel imaging. Probes consist of a pamidronate backbone functionalized with near-infrared fluorophore off the amino terminus of the R_2 side chain. IRDye 800CW carboxylate (LI-COR Biosciences, Lincoln NB. USA) is a nonreactive control probe with similar spectral properties to FRFP750. Unless otherwise noted, standard animal doses of each probe are prepared as 100 nmol/kg in 150 μL of PBS and administered by i.v. tail vein injection.

In vitro binding assays

To create bone powder for in vitro binding assays, several rat forelimbs and hindlimbs were dissected free from soft tissue and cut at the proximal and distal ends, and bone marrow was flushed with distilled water. To defat the bones, specimens were placed in a solution of 1:1 chloroform-methanol for 4 hours and then removed and sonicated in distilled water. Bones were dried, placed in 100% ethanol for 1 hour, and then placed in ethyl ether for 30 minutes. Specimens were dried overnight at 37 °C. Once dry, defatted bone samples were homogenized, producing particles varying from 42 to 295 μm in diameter. Powder was suspended in 0.2 M Tris-formate solution (pH 7.2) and kept at 4 °C.

In vitro dose response

Suspensions of approximately 1.25 mg/mL of bone powder were combined with varying concentrations of FRFP750 (0 to 6 μM) for 1 hour at room temperature in a Millipore 96-well filter plate (Bedford, MA, USA). To separate unbound FRFP from FRFP bound to bone particles in solution, plates were centrifuged at 1000 × *g* for 10 minutes. Eluted, unbound FRFP was collected, and postincubation fluorescence was assessed by plate reader assay (SpectraMax M5, Molecular Devices, Sunnydale, CA, USA). Postincubation fluorescence was compared with preincubation fluorescence to determine the total amount of FRFP bound to bone powder in vitro in relation to a calibrated curve of known FRFP concentrations.

In vitro competitive inhibition

In order for FRFP to be used as a tracer compound for bisphosphonates, it should compete for the same mineral binding sites as unlabeled drug. Competitive inhibition assays were performed comparing FRFP binding in the presence of unlabeled pamidronate (PAM) or alendronate (ALN). As before, 50-μL suspensions of bone powder were mixed with FRFP (1.33 μM) and increasing concentrations of PAM or ALN (0 to 3350 μM; Sigma-Aldrich, St. Louis, MO, USA) for 1 hour at room temperature in a total volume of 100 μL. As before, unbound FRFP was separated, and FRFP bound to bone particles was assessed by comparing pre- and postincubation fluorescence with a calibrated curve of known FRFP concentrations.

In vivo FRFP dose response

To demonstrate the linearity of the in vivo bone fluorescence response to FRFP dose, 7- to 8-week-old male Balb/c mice were administered a range of FRFP (12.5 to 150 nmol/kg, $n = 3$ to 4 per group) by tail vein injection in total volumes of 150 μL, and baseline tissue autofluorescence was compared with that in uninjected controls ($n = 2$). Twenty-four hours after injection, mice were euthanized, and femurs were dissected and imaged by fluorescence reflectance imaging (Maestro Imaging System, Cambridge Research and Instrumentation, Woburn, MA, USA) using 710- to 760-nm bandpass excitation and 810-nm emission at constant exposure. Mean distal femoral fluorescence was assessed within 0.03-cm^2 regions of the bone.

In vivo competitive inhibition

For FRFP to function quantitatively in vivo in the context of a bisphosphonate treatment regime, the treatment dose of

bisphosphonate should not interfere with FRFP binding. To determine whether a surplus of bisphosphonate binding sites exists at relevant skeletal locations, 7- to 8-week-old male Balb/c mice ($n = 3$ per group) were injected with a cocktail of FRFP and increasing concentrations of nonlabeled PAM up to 500× the FRFP concentration. Then 24 hours after injection, mice were euthanized, and femur, tibia, and mandible were dissected into ice-cold Hank's buffered salt solution and kept dark until ex vivo imaging. Ex vivo imaging was performed as done previously, with exposure set to maximize fluorescence per anatomic location while avoiding detector saturation.

To assess fluorescence, distal femoral signal was quantified by measuring a 0.03-cm^2 region of interest centered over the distal femoral growth plate. The proximal tibial signal was assessed by tracing the proximal tibial growth plate from an anterolateral view to measure average fluorescence. In the mandible, a lateral view was assessed for total mandible fluorescence above background. All fluorescence was assessed using ImageJ (National Institutes of Health, Bethesda, MD, USA).

In vivo time course

To determine delivery rate and factors associated with FRFP binding, FRFP750 was administered to the *Brtl/+* mouse, a knock-in model for OI whose type I collagen carries a *COL1A1* Gly349Cys substitution from the mutant allele.[32,33] In this experiment, FRFP was used to assess differences in bisphosphonate delivery between male *Brtl/+* and wild-type mice at 2 and 6 months of age ($n = 6$ to 9 per group). *Brtl/+* mice used in these experiments were offspring from *Brtl/Brtl* × wild-type matings. Following FRFP injection, proximal tibias were shaven and depilated (Nair), and proximal tibial fluorescence was monitored by in vivo noninvasive serial imaging at 2, 6, and 24 hours after injection (Maestro, CRi). An additional group of 6-month-old *Brtl/+* males ($n = 6$) was injected with a comparable dose of the control dye, IRDye 800CW carboxylate (LI-COR Biosciences) and imaged in vivo (Pearl Imager, LI-COR Biosciences) to demonstrate binding specificity of FRFP and washout of the nonbisphosphonate control fluorophore.

At 24 hours, mice were euthanized, and femur, tibia and mandible were dissected and imaged for FRFP delivery. Ex vivo bone fluorescence was assessed as described earlier. Following fluorescent imaging, femurs were imaged by micro–computed tomography (μCT; GE eXplore Locus SP, GE Healthcare, London, Ontario, Canada) and reconstructed at 18-μm voxel size to correlate bone fluorescence with bone surface area in the distal femur. Trabecular bone regions of the distal femur 1.5 to 1.8 mm in length were isolated independent of cortical bone at the growth plate. Bone surface area was assessed using manufacturer-provided software (MicroView ABA 2.2, GE Healthcare).

Long-term FRFP retention

To investigate the ability of FRFP to be used as a long-term marker of bisphosphonate retention, we used 8-week-old male *Brtl/+* mice. The mice were divided into untreated and treated groups ($n = 3$ per group). Untreated mice received two rounds of FRFP injection at 8 (FRFP750) and 9 (FRFP680) weeks of age. Treated mice received identical doses of FRFP but were coinjected with high-dose PAM (7.5 mg/kg) to inhibit bone turnover and prevent removal of FRFP from the bone matrix. At 10 weeks of age, the mice were euthanized, and their limbs were dissected for imaging. To determine percent retention of FRFP750 after 2 weeks in vivo and FRFP680 after 1 week in vivo, two control groups receiving FRFP750 at 8 weeks of age and FRFP680 at 9 weeks of age were euthanized 24 hours after probe injection and analyzed in the same manner as the experimental groups. Treated and untreated bone fluorescence was compared with 8- and 9-week-delivery control values to determine percent of 24-hour dose retained under conditions of normal or downregulated bone turnover.

Histologic analysis

To visualize local FRFP delivery in the mandible, 1× FRFP mandibles were dehydrated, embedded undecalcified in polymethylmethacrylate (PMMA), thick sectioned in a frontal plane using a diamond band saw, and ground to a final section thickness of 50 to 100 μm. Sections were imaged using epifluorescence with a custom near-infrared filter set (excitation 735/50 nm; emission 790/40 nm) on a Zeiss Axiovert system equipped with an iXON+ EMCCD camera (Andor Technology, South Windsor, CT, USA). To visualize FRFP delivery in the femur and tibia, limbs were snap frozen in optimal cutting temperature compound (OCT; Tissue-Tek, Torrance, CA, USA) following dissection, and cryosectioned at 4 to 7 μm (CryoJane Tape Transfer System, Instrumedics, Richmond, IL, USA). Sections were imaged under confocal microscopy (Zeiss LSM 510-META; Carl Zeiss MicroImaging Inc., Thornwood, NY, USA) equipped with a Helium-Neon 2 laser for excitation (633 nm). Following confocal imaging, sections were stained with hematoxylin and eosin and imaged under brightfield microscopy. Confocal and bright-field images were aligned to demonstrate FRFP location.

All animals in this study were maintained and processed in accordance with the NIH *Guide for the Care and Use of Laboratory Animals*.

Statistics

Differences in fluorescence between groups in in vivo competitive inhibition data were assessed by one-way ANOVA. Differences in fluorescence attributed to genotype, treatment, or time in delivery and retention assays were assessed by two-way ANOVA followed by Bonferroni post hoc tests. Statistical significance was assessed at $p < .05$. All data presented as mean ± SD.

Results

In vitro binding assays

FRFP binds to bone particles in solution dose-dependently, with binding saturating at high concentrations (Fig. 1*A*). Scatchard analysis (*inset*) suggests that the maximum FRFP binding in vitro is 2.25 μmol/g of mineral. ALN and PAM were both effective at

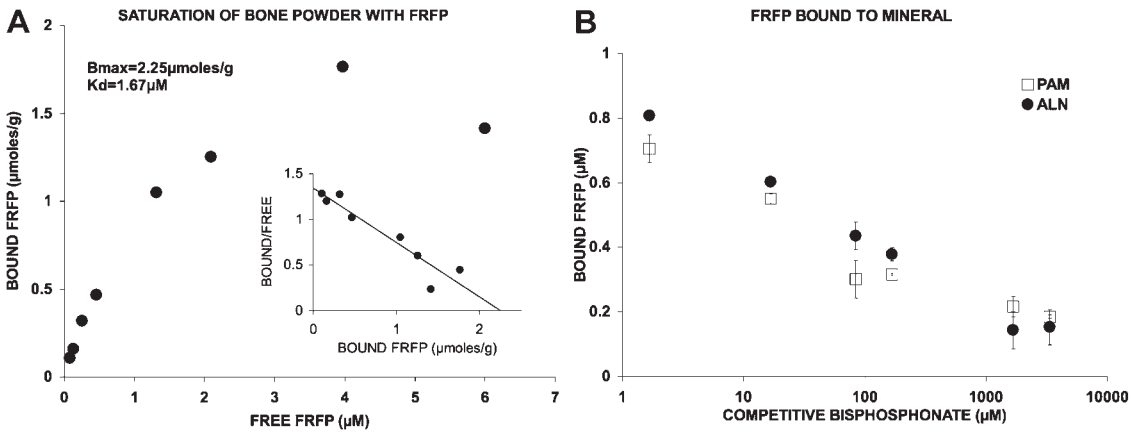

Fig. 1. (*A*) FRFP binds to bone powder dose-dependently and saturates at high doses. (*B*) PAM and ALN both compete FRFP (1.33 μM) away from bone particle suspension.

competing FRFP away from bone powder in an in vitro competitive inhibition assay (Fig. 1*B*).

In vivo FRFP dose response

To demonstrate linear uptake of FRFP in vivo, mice were injected with varying doses of FRFP to monitor linearity of bone fluorescence. Mean fluorescence of the distal femur is linear from approximately 1/8 to 1½ times the imaging dose of 100 nmol/kg (Fig. 2), suggesting a linear reporting of bone fluorescence based on local drug delivery.

In vivo competitive inhibition and localization

In order for FRFP to function effectively as a tracer in vivo in the context of a bisphosphonate treatment regime, the treatment dose of bisphosphonate should not interfere with FRFP binding. In vivo competitive inhibition shows that local delivery of FRFP to the femur, mandible, and tibia is not affected by increasing doses of therapeutic bisphosphonates for concentrations up to 500× FRFP (Fig. 3, one-way ANOVA, no significance detected). In contrast to in vitro competitive inhibition results, where mineral-binding sites are limited by the amount of powder in solution, these data suggest that in vivo, bisphosphonate binding occurs without saturation of mineral-binding sites at the concentrations examined.

FRFP localizes to regions typically associated with high bone turnover, such as the distal femoral growth plate, the femoral head, and the proximal tibial growth plate. In the femur, FRFP is found in bone surrounding the growth plate, in both the metaphysis and epiphysis (Fig. 3*A*). In the mandible, FRFP localizes to the temporomandibular joint and is highly bound in the alveolar bone adjacent to the molars (Fig. 3*B*). Histologic sectioning of the mandible of injected mice reveals widespread FRFP localization (Fig. 4), including the molar, alveolar bone, and incisor root, whereas sections from uninjected animals did not show significant tissue autofluorescence (data not shown). FRFP binding (pseudocolored red) is observed in regions typically affected by ONJ, such as the alveolar bone adjacent to the periodontal ligament (Fig. 4*B*, *D*, *E*) and molar root (Fig. 4*C*). Additional binding is also seen throughout the tooth itself, including the dentin-enamel junction of the incisor (Fig. 4*F*), within the molar dentin space (Fig. 4*G*, ×10), and in what appears to be channels feeding the molar (Fig. 4*H*). This binding may represent vascular sinusoids deficient in endothelial lining cells or a relatively permeable cell junction connection that allows

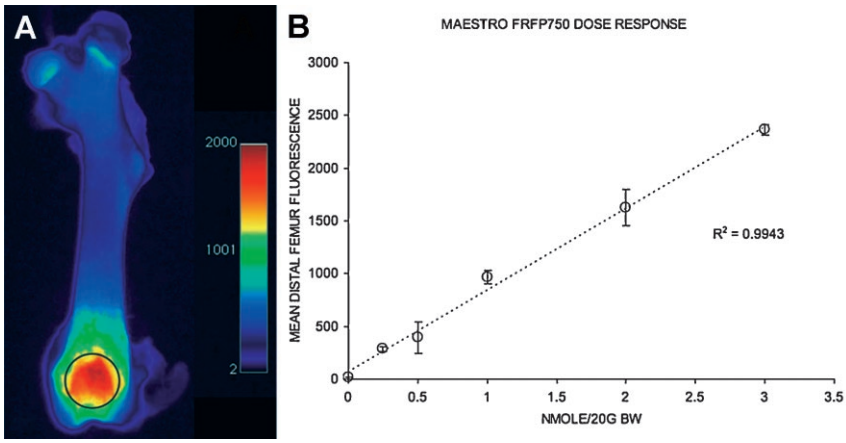

Fig. 2. (*A*) Femoral region of interest chosen for dose-response measures of FRFP delivery. (*B*) Bone fluorescence is linear with administered dose of FRFP.

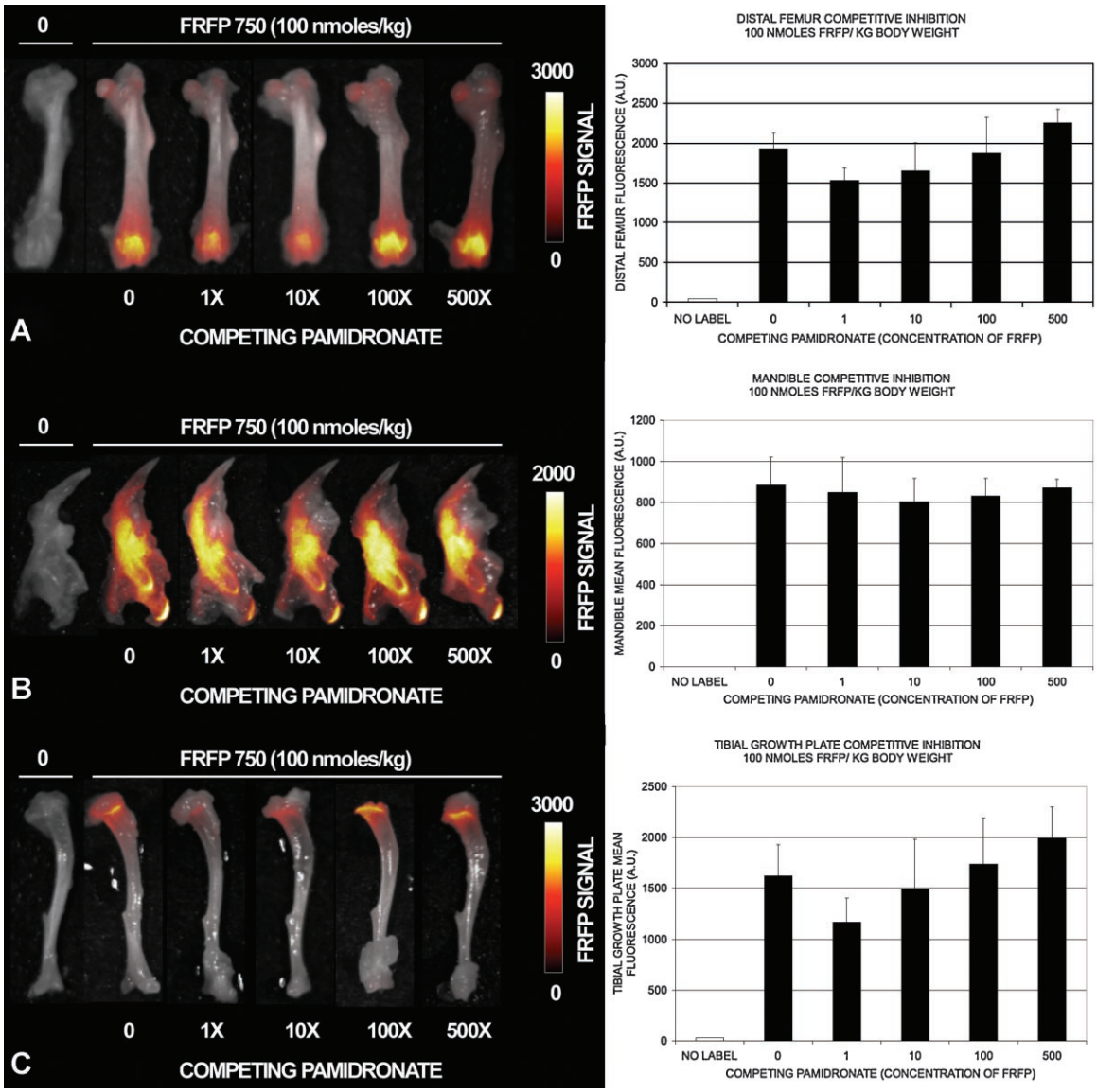

Fig. 3. Competitive inhbition of FRFP with PAM was not found to occur in vivo in the (*A*) femur, (*B*) mandible, or (*C*) tibia, demonstrating no interference between FRFP binding and therapeutic bisphosphonate dosing.

FRFP to penetrate the cell layer and label the mineralized surface surrounding the vasculature.

In vivo time course

Proximal tibial fluorescence was monitored in *Brtl*/+ and wild-type mice at 2, 6, and 24 hours after a single FRFP injection. Consistent with previous studies showing rapid binding of pamidronate to bone,[34] FRFP localizes to the proximal tibia rapidly, with approximately 90% of 24-hour fluorescence occurring within 2 hours of injection (Fig. 5*B*). In contrast, nonbisphosphonate carboxylate control dye clears from the system rapidly, with tibial fluorescence at background levels 24 hours after injection (data not shown).

Tibial fluorescence was marginally but not significantly reduced in 6-month-old *Brtl*/+ mice at all time points studied. Ex vivo distal femoral fluorescence demonstrated that this marginal decrease in femoral fluorescence corresponds to an osteopenic phenotype reflected by μCT analysis (Fig. 5*C*). Plotting femoral fluorescence versus distal femoral bone surface area across age and genotype highlights the dependency of FRFP binding on bone surface area in these animals (Fig. 5*D*).

Long-term FRFP retention

FRFP injected into 8-week-old *Brtl*/+ mice in conjunction with high-dose PAM is significantly retained in bone over 1 and 2 weeks compared with untreated animals (Fig. 6). PAM-treated femurs demonstrate over 100% of the 24-hour control signal, suggesting continued drug delivery after the 24-hour time point, whereas mandibular retention is less than 100% in treated groups, suggesting an altered delivery and retention between groups. Untreated mandibles appear to retain a greater proportion of FRFP than femurs, suggesting a greater retention of bisphosphonate within the mandible. Dual labeling is apparent in both femurs and mandibles, whereas interlabel

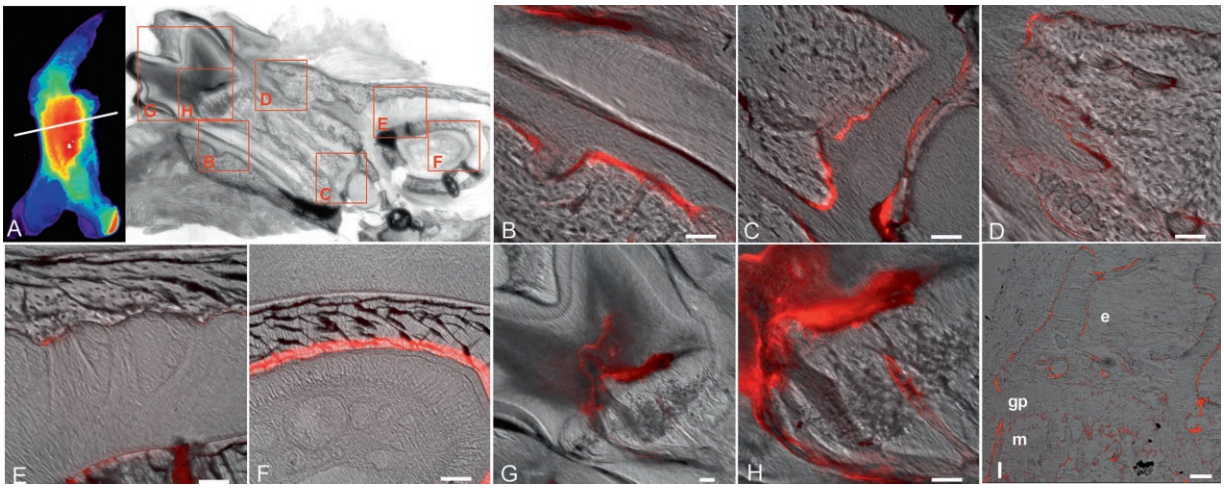

Fig. 4. In situ fluorescence of FRFP signal (*red*) in the mandible demonstrates widespread bisphosphonate localization in regions of concern for ONJ. (*A*) 2.5× overview highlighting location of subsequent 10× (*G*) and 20× panels (*B–F*, *H*). (*Inset*) Whole-mandible fluorescence and location of frontal section. (*B*) Alveolar bone adjacent to periodontal ligament. (*C*) Base of molar root. (*D*) Alveolar bone. (*E*) Bone surrounding incisor periodontal ligament space. (*F*) Incisor dentin-enamel junction. (*G*) ×10 magnification of molar dentin space. (*H*) ×20 magnification of panel *G* showing molar dentin space and supplying vasculature. (*I*) Fluorescence FRFP signal in the proximal femur shows FRFP binding in the epiphyseal (*e*) and metaphyseal (*m*) regions. Growth plate (*gp*) is shown for reference. Scale bar = 50 μm.

distance appears significantly reduced in PAM-treated animals (Fig. 6).

Discussion

After 40 years of development and treatment experience,[35] bisphosphonate usage is expanding beyond traditional low-bone-mass or high-bone-turnover applications to include treatment of pediatric low bone mass[3–6] and is being proposed for use in treating osteonecrosis of the femoral head,[36] stabilization of implant fixation,[37] and the treatment of rheumatoid arthritis.[38] However, several complications have been identified as associated with bisphosphonate treatment, leading, in some cases, to necrosis or unexplained bone failure.[7,19–21] Emerging evidence suggests that bisphosphonates may affect osteoblasts and osteocytes directly, with some studies showing intereference with apoptosis, resulting in prolonged bone formation,[39,40] whereas other studies suggest bisphosphonate toxicity on osteoblasts.[16,41,42] Additionally, the interaction between bisphosphonates and nonbone cells, such as T cells, has been described.[43] Therefore, the development of sensitive techniques to assess local bisphosphonate concentration at relevant skeletal sites would advance understanding of the interplay between bisphosphonates and bone cells in vivo. The data presented here demonstrate that a far-red fluorescent bisphosphonate tracer can be the basis of an imaging strategy for assessing bisphosphonate delivery and retention in vivo.

Delivery of FRFP to the skeleton is rapid, and binding to mineral substrates is consistent with nonlabeled bisphosphonate binding. In vitro, alendronate and pamidronate were comparable in displacing FRFP, consistent with similar binding constants found between these drugs in ^{14}C-labeled bisphosphonate studies.[44] In vivo, nearly 90% of the fluorescent signal from FRFP localized to bone within 2 to 6 hours of injection. This compares favorably with studies of ^{14}C-labeled pamidronate, in which skeletal distribution is rapid initially, slows after 6 hours, and yields peak binding after 24 hours.[34]

Bisphosphonate-mineral binding traditionally has been attributed to the hydroxyl group at the R_1 position off the central P-C-P backbone.[45–48] However, recent evidence points to a role of the R_2 side chain in governing binding as well.[49] In this study, Scatchard plot analysis suggests a maximum binding of 2.25 μmol FRFP per gram of mineral in vitro. Although there is no comparison data for pamidronate binding capacity in the literature, reported alendronate binding capacity is an order of magnitude higher. Sato and colleagues reported alendronate in vitro binding capacity of 100 μmol/g,[50] whereas data extrapolated from Leu and colleagues suggest a binding capacity closer to 10 to 20 μmol/g.[44] Alendronate contains only one additional methyl group on the R_2 side chain compared with pamidronate, and it has a K_i constant similar to that of pamidronate,[44] allowing this comparison to be made. FRFP contains a fluorophore functionalized to the R_2 side chain of pamidronate, which may sterically limit the total amount of FRFP capable of binding to the bone surface and reduce the mineral-binding capacity below that of alendronate.

Our in vivo binding data suggest that FRFP fluorescence depends on the quantity of bone available. More specifically, since FRFP binding appears to be a mineral surface-dependent process,[24] a high linear correlation was observed between distal femoral fluorescence and bone surface area. Injections of up to 14 mg/kg of nonlabeled pamidronate in vivo were unable to compete with FRFP from the bone surface at the concentrations used for imaging. Pamidronate accumulation in the skeleton is linear through at least 30 mg/kg doses,[34] and in vivo bisphosphonate binding-site saturation is suggested to be "practically impossible" in doses used to treat osteoporosis.[51,52] While in vitro competitive inhibition experiments in this study were performed with both pamidronate and alendronate, we only

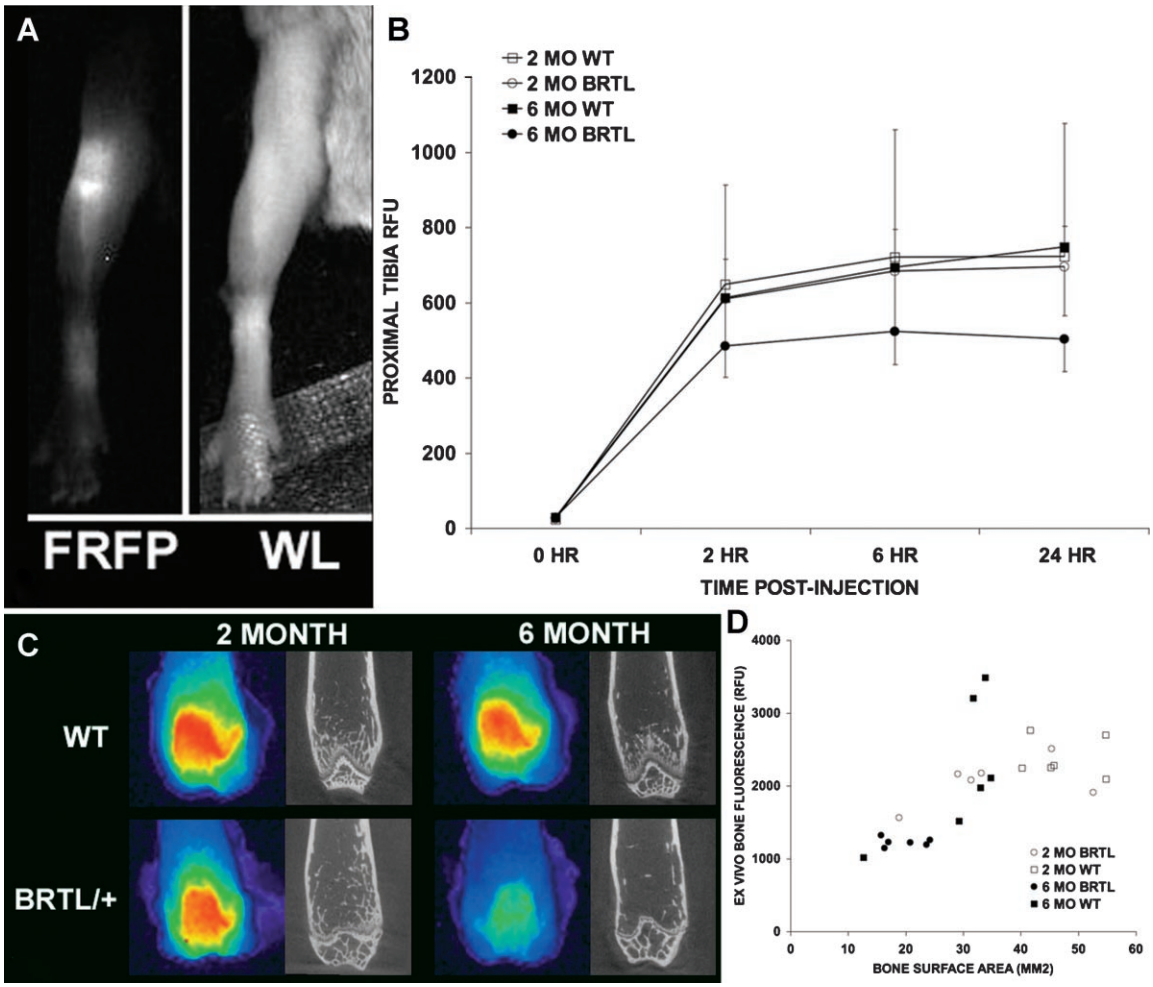

Fig. 5. (*A*) Proximal tibia of *Brtl*/+ and wild-type mice as monitored by in vivo serial imaging over 24 hours. FRFP fluorescent signal is shown (*FRFP*) with corresponding white-light reference image (*WL*). (*B*) Delivery of FRFP is rapid, with nearly 90% of 24-hour dose delivered within 2 hours. Six-month-old *Brtl*/+ tibias demonstrate reduced fluorescence versus wild-type and 2-month-old *Brtl*/+ animals. (*C*) Ex vivo imaging of femurs from 2- and 6-month-old *Brtl*/+ and wild-type mice demonstrates a reduction in distal femoral fluorescence that corresponds to osteopenia noted in μCT cross sections. (*D*) Distal femoral fluorescence is linearly correlated with total distal femoral bone surface area, suggesting that FRFP, like bisphosphonates, binds in a bone surface–mediated manner.

performed in vivo competitive inhibition with pamidronate. However, similar findings could be inferred based on results suggesting that saturation of alendronate in the skeleton occurs only at high doses, when single i.v. injections exceed 10 mg/kg.[53] Therefore, because tracer doses of FRFP at the concentrations used in this study are small compared with such saturation doses, our data suggest that FRFP can be used in conjunction with bisphosphonate treatment in vivo without interfering with FRFP signal at the low concentration used here.

In this study, aged *Brtl* mice with low bone mass in the distal femur showed correspondingly low FRFP delivery to those regions, corroborating the dependence of bisphosphonate delivery, at least in part, on the number of mineralized surfaces available for drug binding. In a clinical study of pamidronate treatment in children with types III and IV OI, significant variability existed in the individual response of patients to treatment.[54] Our current data suggests that existing bone mass may play an important role in determining local concentration and thus possibly effectiveness of antiresorptives in vivo. This contrasts with evidence suggesting that among postmenopausal women treated with once-weekly bisphosphonates, nonresponders to the drug were likely to have a higher baseline trochanteric bone mineral density.[55] Therefore, factors in addition to bone mass, including local vascular delivery and local bone turnover rates, likely play a role in determining the effectiveness of bisphosphonate treatment for low bone mass.

Animals labeled with FRFP for 1 and 2 weeks demonstrate fluorescence retention that correlates with local bone turnover conditions. In animals cotreated with therapeutic doses of pamidronate, fluorescence signal is preserved throughout the 2 weeks, whereas fluorescence decreases significantly in untreated animals. The prolonged retention and fluorescence of local FRFP in a low-bone-turnover condition suggests that changes in FRFP signal may be used as a surrogate marker for turnover of labeled bone in the presence or absence of treatment doses of bisphosphonate.

At 6 months, *Brtl* mice had a reduced bone-formation rate compared with wild-type mice, which also may contribute to

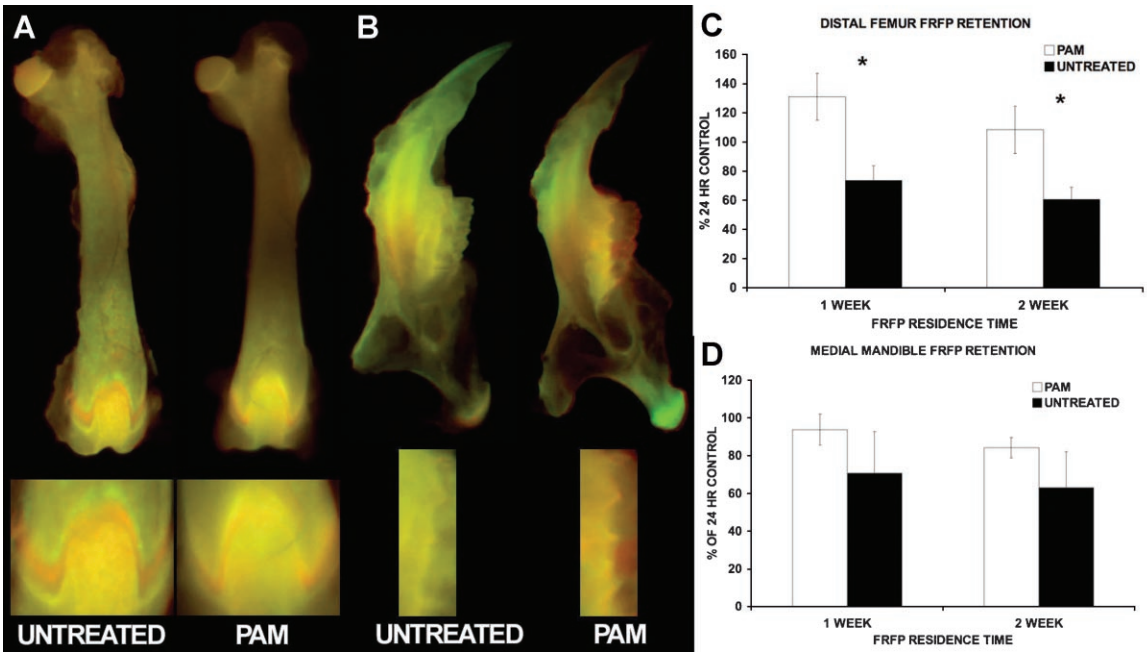

Fig. 6. FRFP retention in untreated and PAM-treated animals after 1 (*red*) and 2 (*green*) weeks in vivo in femur (*A*) and mandible (*B*). (*C*, *D*) Percent signal retention derived by normalizing 1- and 2-week signal by specimens assayed 24 hours after FRFP delivery.

reduced bisphosphonate delivery.[56] Conversely, high levels of bone turnover may play a role in clearing the skeleton of deposited bisphosphonate. Pamidronate has been detected in the urine of OI patients 8 years following cessation of treatment,[22] suggesting that despite local bisphosphonate concentration, drug still can be turned over in the body as osteoclasts attempt to remodel treated bone. Using FRFP as a tracer compound for bisphosphonate retention will allow for long-term analysis of site-specific turnover of drug in vivo. Additionally, turnover is often inversely correlated with mineral crystal size. As crystalline size decreases, the specific surface area will increase, potentially allowing for greater bisphosphonate binding within a given region of bone. While not investigated in this study, FRFP fluorescence may provide insight into local mineral crystal size based on available bisphosphonate binding sites. Crystal size is governed by many factors, including age, collagen and noncollagenous template, diet, and disease,[57] and crystalline size and purity may be associated with fracture risk independent of differences in bone mass.[58,59] Therefore, understanding whether local bisphosphonate concentration is governed by mineral crystal size may be important in understanding treatment for other bone disorders.

Together these data suggest that FRFP imaging is a viable technique to monitor the delivery and retention of bisphosphonates in vivo. This study was performed using a fluorescent pamidronate analogue. While different bisphosphonates have different binding affinities and interactions with hydroxyapatite,[49] to date, we are unaware of studies that demonstrate heterogeneous site-specific binding of different bisphosphonates to different anatomic locations. Given this, FRFP can be used to monitor factors such vascular delivery and available binding surfaces independent of bisphosphonate type. Other fluorescent bisphosphonate analogues have been described[30] but have not yet been tested against FRFP to determine whether heterogeneous site-specific binding of different bisphosphonates occurs.

This technique will be useful for examining side effects that have been associated with bisphosphonate treatment. Bisphosphonates have been used to treat low bone mass found in osteogenesis imperfecta for over 15 years.[60] Intravenous bisphosphonate therapy produces positive gains in vertebral morphology and bone mineral density in children with osteogenesis imperfecta.[54,61–63] However, in controlled studies of bisphosphonate treatment in osteogenesis imperfecta, no difference has been found in nonvertebral fracture rates in patients given oral alendronate, intravenous neridronate, or pamidronate.[64] This site specificity of effectiveness may relate to site-specific differences in bisphosphonate delivery or retention in vivo. This study demonstrates heterogeneous bisphosphonate distribution among skeletal locations, suggesting that regions of highest bone turnover may experience the highest rate of drug delivery but also may be susceptible to high rates of drug removal depending on applied dose.

The characteristic radiographic feature of bisphosphonate treatment in a growing skeleton is the metaphyseal banding patterns originating at the growth plate and extending through the metaphysis into the diaphysis as the patient grows.[6,12–14,23] The intensity, timing, and spacing of these lines correlate with the dose and frequency of bisphosphonate delivery and suggest regions of unresorbed bone and/or calcified cartilage resulting from altered growth plate remodeling.[23] A similar pattern of deposition and spacing of FRFP during treatment suggests that these sclerotic areas contain high local bisphosphonate concentration. The long-term functional implication of this finding is unclear. While these sclerotic lines add material to an osteopenic bone, the orientation of these bands may not be

consistent with the primary loading direction of the bone. It is also possible that these regions may act as stress risers, and a case report has described fractures at one such site when treatment was halted prior to fusion of the growth plate.[15] The combination of high stress plus high concentration of antiresorptive drug may make these locations prone to accumulated fatigue damage incapable of normal tissue repair over time. Bisphosphonate treatment has been shown to delay tooth eruption in treated OI children, presumably by interfering with osteoclast-mediated bone remodeling or tooth root development.[11] While this study did not focus specifically on tooth development, we noted significant FRFP localization within both mandibular bone and tooth structures. FRFP was found in the vascular channels supplying the molars, within the molar dentin space, and at the dentin-enamel junction of the incisor. Additionally, FRFP localized in the alveolar bone adjacent to the periodontal ligaments and molar roots. These are regions of bone that may be associated with the thickened alveolar bone and regions of necrotic bodies that have been found in the mandible in patients with osteonecrosis of the jaw.[65] High levels of an antiresorptive in the oral cavity may induce low bone turnover, resulting in decreased blood flow, bone cell necrosis, and cellular apoptosis, mechanisms that have been proposed to be responsible for the nonhealing lesions typical of ONJ.[20] This imaging strategy may be useful to pursue these hypotheses by directly visualizing bisphosphonate delivery and retention in relevant skeletal sites.

The usefulness of FRFP as a biomarker for bisphosphonate delivery and retention in vivo is bolstered by parallel studies between FRFP and radiolabeled bisphosphonates. FRFP has been used to visualize osteogenic labeling in bone-defect models, with high fluorescence concentrating in areas of high osteoblastic activity.[24,26] These studies corroborate earlier studies using radiolabeled bisphosphonates to demonstrate high drug delivery to sites of active bone regeneration during fracture repair[66] and histologic studies demonstrating unremodeled cartilage retained in fracture callus treated with bisphosphonate.[67] Similarly, FRFP, when injected into mice with osteolytic lesions resulting from tumor xenograft injections, localizes under osteoclasts at the tumor-bone interface.[24] Bisphosphonates have long been described as localizing underneath osteoclasts, and fluorescent bisphosphonate strategies have been used to visualize osteoclastic uptake of drug during bone resorption.[30]

Near-infrared contrast agents are less attenuated by overlying tissue than similar green-shifted probes.[31] However, while near-infrared signals can propagate between 5 and 12 cm through soft tissues,[68] using the fluorescence reflectance imaging described in this study, signals are still surface-weighted[69] and may be limited to penetration depths of less than 1 cm.[70] Therefore, when performing any type of fluorescence imaging, choice of anatomic location is critical. In this study, we imaged in vivo proximal tibial FRFP signal owing to ease of imaging at this anatomic location and relatively low tissue coverage. However, we also imaged ex vivo distal femoral FRFP signal from the same animals, and signals from these two locations were highly linearly correlated ($r^2 = 0.63$, $p < .0001$). Femoral, mandibular, and tibial specimens all were imaged ex vivo to allow better visualization of signal without overlying tissue. Advances in optical imaging technology continue to improve on quantitative fluorescence imaging. Fluorescence molecular tomography (FMT) is less dependent on depth of signal than fluorescence reflectance imaging[69,70] and has been used to visualize and quantify FRFP and similar near-infrared probes in vivo within the skeleton.[26,71] Further advances will continue to widen options for using agents such as FRFP for in vivo imaging of biologic activity.

In conclusion, fluorescent bisphosphonate imaging is a valid technique for visualizing site-specific bisphosphonate delivery and retention in vivo. Small tracer doses are delivered rapidly in the skeleton and can be used in the context of a standard bisphosphonate treatment regime without interfering with drug binding. FRFP binding relies on local bone surface area, and removal of tracer probe is reflected in animals undergoing increased bone turnover. Combining fluorescent bisphosphonates with other fluorescent markers of osteoblastic,[72] osteocytic,[73] or osteoclastic[71] markers will facilitate in vivo and histologic imaging studies to investigate models of osteoporosis, osteogenesis imperfecta, and osteonecrosis of the jaw, where drug-cell interactions leading to a positive or negative outcome have yet to be described.

Disclosures

All the authors state that they have no conflicts of interest.

Acknowledgments

We gratefully acknowledge Xixi Wang and Bonnie Nolan for assistance with animal experiments; Jaclynn Kreider, Ben Sinder, Logan White, and John Foo for technical assistance; and Dr Steve Goldstein for thoughtful discussion.

References

1. Rodan GA, Martin TJ. Therapeutic approaches to bone diseases. Science. 2000;289:1508–1514.
2. Russell RG, Rogers MJ. Bisphosphonates: from the laboratory to the clinic and back again. Bone. 1999;25:97–106.
3. Hickey J, Lemons D, Waber P, Seikaly MG. Bisphosphonate use in children with bone disease. J Am Acad Orthop Surg. 2006;14:638–644.
4. Ramachandran M, Ward K, Brown RR, Munns CF, Cowell CT, Little DG. Intravenous bisphosphonate therapy for traumatic osteonecrosis of the femoral head in adolescents. J Bone Joint Surg Am. 2007;89: 1727–1734.
5. Sholas MG, Tann B, Gaebler-Spira D. Oral bisphosphonates to treat disuse osteopenia in children with disabilities: a case series. J Pediatr Orthop. 2005;25:326–331.
6. Glorieux FH, Bishop NJ, Plotkin H, Chabot G, Lanoue G, Travers R. Cyclic administration of pamidronate in children with severe osteogenesis imperfecta. N Engl J Med. 1998;339:947–952.
7. Neviaser AS, Lane JM, Lenart BA, Edobor-Osula F, Lorich DG. Low-energy femoral shaft fractures associated with alendronate use. J Orthop Trauma. 2008;22:346–350.
8. Boskey AL, Spevak L, Weinstein RS. Spectroscopic markers of bone quality in alendronate-treated postmenopausal women. Osteoporos Int. 2009;20:793–800.

9. Durchschlag E, Paschalis EP, Zoehrer R, et al. Bone material properties in trabecular bone from human iliac crest biopsies after 3- and 5-year treatment with risedronate. J Bone Miner Res. 2006;21:1581–1590.
10. Munns CF, Rauch F, Zeitlin L, Fassier F, Glorieux FH. Delayed osteotomy but not fracture healing in pediatric osteogenesis imperfecta patients receiving pamidronate. J Bone Miner Res. 2004;19:1779–1786.
11. Kamoun-Goldrat A, Ginisty D, Le Merrer M. Effects of bisphosphonates on tooth eruption in children with osteogenesis imperfecta. Eur J Oral Sci. 2008;116:195–198.
12. Grissom LE, Harcke HT. Radiographic features of bisphosphonate therapy in pediatric patients. Pediatr Radiol. 2003;33:226–229.
13. Rauch F, Travers R, Munns C, Glorieux FH. Sclerotic metaphyseal lines in a child treated with pamidronate: histomorphometric analysis. J Bone Miner Res. 2004;19:1191–1193.
14. van Persijn van Meerten EL, Kroon HM, Papapoulos SE. Epi- and metaphyseal changes in children caused by administration of bisphosphonates. Radiology. 1992;184:249–254.
15. Rauch F, Cornibert S, Cheung M, Glorieux FH. Long-bone changes after pamidronate discontinuation in children and adolescents with osteogenesis imperfecta. Bone. 2007;40:821–827.
16. Uveges T, Kozloff KM, Ty JM, et al. Alendronate treatment of Brtl osteogenesis imperfecta mouse improves femoral geometry and load response before fracture but has detrimental effects on osteoblasts and bone formation and decreases predicted material properties. Journal of Bone and Mineral Research. 2009;24:849–859.
17. American Association of Oral and Maxillofacial Surgeons position paper on bisphosphonate-related osteonecrosis of the jaws. J Oral Maxillofac Surg. 2007;65:369–376.
18. Khosla S, Burr D, Cauley J, et al. Bisphosphonate-associated osteonecrosis of the jaw: report of a task force of the American Society for Bone and Mineral Research. J Bone Miner Res. 2007;22:1479–1491.
19. Marx RE. Pamidronate (Aredia) and zoledronate (Zometa) induced avascular necrosis of the jaws: a growing epidemic. J Oral Maxillofac Surg. 2003;61:1115–1117.
20. Rizzoli R, Burlet N, Cahall D, et al. Osteonecrosis of the jaw and bisphosphonate treatment for osteoporosis. Bone. 2008;42:841–847.
21. Ruggiero SL, Mehrotra B, Rosenberg TJ, Engroff SL. Osteonecrosis of the jaws associated with the use of bisphosphonates: a review of 63 cases. J Oral Maxillofac Surg. 2004;62:527–534.
22. Papapoulos SE, Cremers SC. Prolonged bisphosphonate release after treatment in children. N Engl J Med. 2007;356:1075–1076.
23. Al Muderis M, Azzopardi T, Cundy P. Zebra lines of pamidronate therapy in children. J Bone Joint Surg Am. 2007;89:1511–1516.
24. Kozloff KM, Weissleder R, Mahmood U. Non-invasive optical detection of bone mineral. J Bone Miner Res. 2007;22:1208–1216.
25. Zaheer A, Lenkinski RE, Mahmood A, Jones AG, Cantley LC, Frangioni JV. In vivo near-infrared fluorescence imaging of osteoblastic activity. Nat Biotechnol. 2001;19:1148–1154.
26. Zilberman Y, Kallai I, Gafni Y, et al. Fluorescence molecular tomography enables in vivo visualization and quantification of nonunion fracture repair induced by genetically engineered mesenchymal stem cells. J Orthop Res. 2008;26:522–530.
27. Lenkinski RE, Ahmed M, Zaheer A, Frangioni JV, Goldberg SN. Near-infrared fluorescence imaging of microcalcification in an animal model of breast cancer. Acad Radiol. 2003;10:1159–1164.
28. Aikawa E, Nahrendorf M, Figueiredo JL, et al. Osteogenesis associates with inflammation in early-stage atherosclerosis evaluated by molecular imaging in vivo. Circulation. 2007;116:2841–2850.
29. Figueiredo JL, Passerotti CC, Sponholtz T, Nguyen HT, Weissleder R. A novel method of imaging calcium urolithiasis using fluorescence. J Urol. 2008;179:1610–1614.
30. Coxon FP, Thompson K, Roelofs AJ, Ebetino FH, Rogers MJ. Visualizing mineral binding and uptake of bisphosphonate by osteoclasts and non-resorbing cells. Bone. 2008;42:848–860.
31. Weissleder R, Ntziachristos V. Shedding light onto live molecular targets. Nat Med. 2003;9:123–128.
32. Forlino A, Porter FD, Lee EJ, Westphal H, Marini JC. Use of the Cre/lox recombination system to develop a non-lethal knock-in murine model for osteogenesis imperfecta with an a1(I) G349C substitution. Variability in phenotype in BrtlIV mice. J Biol Chem. 1999;274:37923–37931.
33. Kozloff KM, Carden A, Bergwitz C, et al. Brittle IV mouse model for osteogenesis imperfecta IV demonstrates postpubertal adaptations to improve whole bone strength. J Bone Miner Res. 2004;19:614–622.
34. Hoggarth CR, Bennett R, Daley-Yates PT. The pharmacokinetics and distribution of pamidronate for a range of doses in the mouse. Calcif Tissue Int. 1991;49:416–420.
35. Fleisch H, Russell RG, Francis MD. Diphosphonates inhibit hydroxyapatite dissolution in vitro and bone resorption in tissue culture and in vivo. Science. 1969;165:1262–1264.
36. Little DG, Peat RA, McEvoy A, Williams PR, Smith EJ, Baldock PA. Zoledronic acid treatment results in retention of femoral head structure after traumatic osteonecrosis in young Wistar rats. J Bone Miner Res. 2003;18:2016–2022.
37. Tanzer M, Karabasz D, Krygier JJ, Cohen R, Bobyn JD. The Otto Aufranc Award: bone augmentation around and within porous implants by local bisphosphonate elution. Clin Orthop Relat Res. 2005;441:30–39.
38. Jarrett SJ, Conaghan PG, Sloan VS, et al. Preliminary evidence for a structural benefit of the new bisphosphonate zoledronic acid in early rheumatoid arthritis. Arthritis Rheum. 2006;54:1410–1414.
39. Plotkin LI, Lezcano V, Thostenson J, Weinstein RS, Manolagas SC, Bellido T. Connexin 43 is required for the anti-apoptotic effect of bisphosphonates on osteocytes and osteoblasts in vivo. J Bone Miner Res. 2008;23:1712–1721.
40. Plotkin LI, Weinstein RS, Parfitt AM, Roberson PK, Manolagas SC, Bellido T. Prevention of osteocyte and osteoblast apoptosis by bisphosphonates and calcitonin. J Clin Invest. 1999;104:1363–1374.
41. Iwata K, Li J, Follet H, Phipps RJ, Burr DB. Bisphosphonates suppress periosteal osteoblast activity independently of resorption in rat femur and tibia. Bone. 2006;39:1053–1058.
42. Nakamura M, Udagawa N, Matsuura S, et al. Osteoprotegerin regulates bone formation through a coupling mechanism with bone resorption. Endocrinology. 2003;144:5441–5449.
43. Kunzmann V, Bauer E, Feurle J, Weissinger F, Tony HP, Wilhelm M. Stimulation of gammadelta T cells by aminobisphosphonates and induction of antiplasma cell activity in multiple myeloma. Blood. 2000;96:384–392.
44. Leu CT, Luegmayr E, Freedman LP, Rodan GA, Reszka AA. Relative binding affinities of bisphosphonates for human bone and relationship to antiresorptive efficacy. Bone. 2006;38:628–636.
45. Francis MD, Ferguson DL, Tofe AJ, Bevan JA, Michaels SE. Comparative evaluation of three diphosphonates: in vitro adsorption (C- 14 labeled) and in vivo osteogenic uptake (Tc-99m complexed). J Nucl Med. 1980;21:1185–1189.
46. Jung A, Bisaz S, Fleisch H. The binding of pyrophosphate and two diphosphonates by hydroxyapatite crystals. Calcif Tissue Res. 1973;11:269–280.
47. Mitterhauser M, Toegel S, Wadsak W, et al. Binding studies of [18F]-fluoride and polyphosphonates radiolabelled with [99mTc], [111In], [153Sm] and [188Re] on bone compartments: Verification of the pre vivo model? Bone. 2005;37:404–412.
48. van Beek E, Hoekstra M, van de Ruit M, Lowik C, Papapoulos S. Structural requirements for bisphosphonate actions in vitro. J Bone Miner Res. 1994;9:1875–1882.

49. Nancollas GH, Tang R, Phipps RJ, et al. Novel insights into actions of bisphosphonates on bone: differences in interactions with hydroxyapatite. Bone. 2006;38:617–627.
50. Sato M, Grasser W, Endo N, et al. Bisphosphonate action. Alendronate localization in rat bone and effects on osteoclast ultrastructure. J Clin Invest. 1991;88:2095–2105.
51. Cremers SC, Papapoulos SE, Gelderblom H, et al. Skeletal retention of bisphosphonate (pamidronate) and its relation to the rate of bone resorption in patients with breast cancer and bone metastases. J Bone Miner Res. 2005;20:1543–1547.
52. Masarachia P, Weinreb M, Balena R, Rodan GA. Comparison of the distribution of 3H-alendronate and 3H-etidronate in rat and mouse bones. Bone. 1996;19:281–290.
53. Lin JH, Chen IW, Duggan DE. Effects of dose, sex, and age on the disposition of alendronate, a potent antiosteolytic bisphosphonate, in rats. Drug Metab Dispos. 1992;20:473–478.
54. Letocha AD, Cintas HL, Troendle JF, et al. Controlled trial of pamidronate in children with types III and IV osteogenesis imperfecta confirms vertebral gains but not short-term functional improvement. J Bone Miner Res. 2005;20:977–986.
55. Burnett-Bowie SM, Saag K, Sebba A, et al. Prediction of changes in bone mineral density in postmenopausal women treated with once-weekly bisphosphonates. J Clin Endocrinol Metab. 2009;94:1097–1103.
56. Uveges TE, Collin-Osdoby P, Cabral WA, et al. Cellular mechanism of decreased bone in Brtl mouse model of OI: Imbalance of decreased osteoblast function and increased osteoclasts and their precursors. J Bone Miner Res. 2008;23:1983–1994.
57. Boskey AL. Bone mineral crystal size. Osteoporos Int. 2003;14(Suppl 5): S16-20; discussion S20-1.
58. Gourion-Arsiquaud S, Faibish D, Myers E, et al. Use of FTIR spectroscopic imaging to identify parameters associated with fragility fracture. J Bone Miner Res. 2009;24:1565–1571.
59. McCreadie BR, Morris MD, Chen TC, et al. Bone tissue compositional differences in women with and without osteoporotic fracture. Bone. 2006;39:1190–1195.
60. Marini JC. Bone: Use of bisphosphonates in children-proceed with caution. Nat Rev Endocrinol. 2009;5:241–243.
61. Gatti D, Antoniazzi F, Prizzi R, et al. Intravenous neridronate in children with osteogenesis imperfecta: a randomized controlled study. J Bone Miner Res. 2005;20:758–763.
62. Rauch F, Munns CF, Land C, Cheung M, Glorieux FH. Risedronate in the treatment of mild pediatric osteogenesis imperfecta: a randomized placebo-controlled study. J Bone Miner Res. 2009;24:1282–1289.
63. Sakkers R, Kok D, Engelbert R, et al. Skeletal effects and functional outcome with olpadronate in children with osteogenesis imperfecta: a 2-year randomised placebo-controlled study. Lancet. 2004;363: 1427–1431.
64. Marini JC. Should children with osteogenesis imperfecta be treated with bisphosphonates? Nat Clin Pract Endocrinol Metab. 2006;2: 14–15.
65. Barragan-Adjemian C, Lausten L, Ang DB, Johnson M, Katz J, Bonewald LF. Bisphosphonate-related osteonecrosis of the jaw: model and diagnosis with cone beam computerized tomography. Cells Tissues Organs. 2009;189:284–288.
66. Li J, Mori S, Kaji Y, Kawanishi J, Akiyama T, Norimatsu H. Concentration of bisphosphonate (incadronate) in callus area and its effects on fracture healing in rats. J Bone Miner Res. 2000;15:2042–2051.
67. Gerstenfeld LC, Sacks DJ, Pelis M, et al. Comparison of effects of the bisphosphonate alendronate versus the RANKL inhibitor denosumab on murine fracture healing. J Bone Miner Res. 2009;24:196–208.
68. Ntziachristos V, Tung CH, Bremer C, Weissleder R. Fluorescence molecular tomography resolves protease activity in vivo. Nat Med. 2002;8:757–760.
69. Montet X, Figueiredo JL, Alencar H, Ntziachristos V, Mahmood U, Weissleder R. Tomographic fluorescence imaging of tumor vascular volume in mice. Radiology. 2007;242:751–758.
70. Ntziachristos V, Bremer C, Graves EE, Ripoll J, Weissleder R. In vivo tomographic imaging of near-infrared fluorescent probes. Mol Imaging. 2002;1:82–88.
71. Kozloff KM, Quinti L, Patntirapong S, et al. Non-invasive optical detection of cathepsin K-mediated fluorescence reveals osteoclast activity in vitro and in vivo. Bone. 2009;44:190–198.
72. Kalajzic I, Kalajzic Z, Kaliterna M, et al. Use of type I collagen green fluorescent protein transgenes to identify subpopulations of cells at different stages of the osteoblast lineage. J Bone Miner Res. 2002;17:15–25.
73. Dallas SL, Veno PA, Rosser JL, et al. Time lapse imaging techniques for comparison of mineralization dynamics in primary murine osteoblasts and the late osteoblast/early osteocyte-like cell line MLO-A5. Cells Tissues Organs. 2009;189:6–11.